

Electrochemical Sensor Based on Nafion/Gold Nanoparticle/Electrochemically Reduced Graphene Oxide Composite-Modified Glassy Carbon Electrode for the Detection of Diuron

Jianfang Qin*, YingLian Qin, Xiuping Jiang, Yajin Du, Yajing Du, Chen-Zhong Yao, Xi Wang, Haiying Yang*

Department of Chemistry, Yuncheng University, Yuncheng, 044300, PR China

*E-mail: jianfangqin2006@163.com (J. Qin), haiyingyang79@hotmail.com (H. Yang)

Received: 18 June 2020 / Accepted: 5 September 2020 / Published: 30 September 2020

A novel sensitive electrochemical sensor based on a glassy carbon electrode (GCE) modified with a Nafion/gold nanoparticle/electrochemically reduced graphene oxide (Nafion/AuNPs/RGO) composite membrane was applied to detect diuron. The Nafion/AuNPs/RGO composites with the advantages of a large surface area, specific binding sites and a faster electron transfer rate were analysed. The synergistic effects of the RGO and AuNPs composites and the effective absorption of diuron resulted in a high interfacial conductivity. Therefore, the fabricated sensor showed excellent performance. The electrode exhibited a linear response from 1.0×10^{-12} M to 1.0×10^{-9} M for diuron and a detection limit of 4.1×10^{-13} M under the optimized conditions. Accordingly, reproducibility, stability and anti-interference tests were carried out. Furthermore, the designed sensor was utilized to detect diuron in real samples to evaluate the accuracy of the method. The recovery of diuron was 91.2%-108.2%. This approach provides a new avenue for the sensitive detection of diuron in practical applications.

Keywords: AuNPs; RGO; differential pulse voltammetry; synergistic effects; practical application.

1. INTRODUCTION

Diurons are broadly employed in agricultural pesticides, which are used for growing sugar cane, fruits, cotton, etc. [1]. Diuron has a harmful effect on humans and other living creatures. It is necessary to monitor its level in the environment. Various analytical methods for the accurate determination of diuron, including electrochemistry [2,3], chromatography [4], high-pressure liquid chromatography [5], capillary electrophoresis [6,7], fluorimetry [8] and spectrophotometry [9], have been surveyed. Compared to other analytical techniques, electrochemical sensors are a simple and reliable method for the detection of contaminants and offers advantages, such as low cost and easy operation [10,11].

Reduced graphene oxide (RGO) has superior conductivity, good loading capacity and large surface area [12]. Hence, it can be adopted widely for constructing sensors.

Gold nanoparticles (AuNPs) have advantages, such as a fast electron transfer rate, good biocompatibility and high catalytic activity [13]. Immobilizing AuNPs onto RGO prevents the aggregation of RGO, increases the surface-to-volume ratio and includes particular binding sites [14]. Benefitting from its high affinity towards cations, chemical inertness and excellent antifouling capacity, Nafion is a very suitable material to modify RGO by means of its oxygen-functional groups and stabilize RGO in solution [15].

Herein, we propose a novel electrochemical sensor based on Nafion/AuNPs/RGO/GCE for the sensitive determination of diuron.

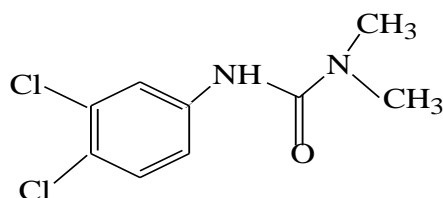


Figure 1. Structure of diuron

2. EXPERIMENTAL SECTION

2.1. Reagents and solutions

Graphite oxides (GO) were supplied by Xianfeng Nanomaterials Technology Co., Ltd. (Nanjing, China). Diuron, H₂AuCl₄, and Nafion (5%) were obtained from Sigma–Aldrich. A 0.1 M phosphate buffer solution (PBS) was prepared with NaH₂PO₄·2H₂O and Na₂HPO₄·12H₂O. The diuron solution was prepared in 15% ethyl alcohol. All reagents used were analytical-grade. Double-distilled water was used throughout the experiments.

2.2. Apparatus

SEM images were obtained by scanning electron microscopy (SEM Hitachi S-4800 microscope, Japan). A CHI-660 electrochemical workstation equipped with a traditional three-electrode system (Chenhua Instruments Co., Shanghai, China) was used, which was composed of the designed electrochemical sensor as the working electrode, a platinum wire as the counter electrode, and Ag/AgCl as the reference electrode [8].

2.3. Fabrication of the electrochemical sensor

Suspensions were prepared in deionized water by mild ultrasonication for 1 h to ensure homogeneous dispersion. The glassy carbon electrode (GCE) was smoothed using aqueous alumina slurry (0.05 μm) and washed completely to acquire a clean surface. A 5 μL suspension of GO was dropped on a clean GCE and dried at room temperature, resulting in the GO/GCE electrode. Next, the GO/GCE was immersed into pH=7.32 M PBS solution at a fixed potential of -0.9 V for 400 s to transform GO to RGO. Then, the AuNPs were electrodeposited onto the RGO/GCE electrode in a 3.0

mM HAuCl_4 solution at an immobile potential of -0.2 V for 400 s, resulting in the AuNPs/RGO/GCE electrode. Finally, 4 μL of 0.5% Nafion was dropped on the surface of the electrode, resulting in the final Nafion/AuNPs/RGO/GCE electrode. After each step, the electrode was washed completely and dried. For comparison, GO/GCE, RGO/GCE and AuNPs/RGO/GCE were prepared using the same method.

2.4. Experimental procedure

Cyclic voltammetry curves (CV) and electrochemical impedance spectroscopy (EIS) were measured in 0.1 M PBS containing 0.1 M KCl. The potential range of CV was from -0.2 V to 0.8 V, and the scan rate was 0.1 V/s. The frequency range of EIS was from 100000 Hz to 0.1 Hz with a signal amplitude of 5 mV. The detection of diuron using differential pulse voltammetry (DPV) was acquired in the potential range of 0.70 V to 1.40 V at a scan rate of 0.1 V/s in 0.1 M pH 4.5 PBS.

3. RESULTS AND DISCUSSION

3.1 Characterization of the sensor

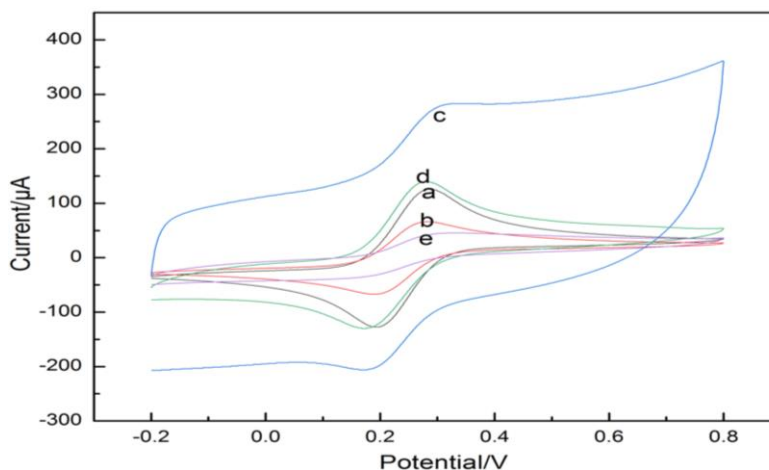


Figure 2. CV curves of the (a) bare GCE, (b) GO/GCE, (c) RGO/GCE, (d) AuNPs/RGO/GCE, (e) Nafion/AuNPs/RGO/GCE electrode in 5.0 mM $[\text{Fe}(\text{CN})_6]^{3-/4-}$.

The fabrication process of various modified electrodes was suggested by using CV and EIS as redox labels. The results are shown in Fig. 2 and Fig. 3. To obtain the EIS curves, a Randle equivalent circuit was selected (Fig. 3B). As shown in Fig. 2, the electrochemical activity of the redox peaks and the peak potential separation (ΔE) were 0.094 V (curve a). In curve b, the oxidation peak current was lower than that in curve a, indicating that the electron transfer of $[\text{Fe}(\text{CN})_6]^{3-/4-}$ was impeded. On the other hand, compared to GO/GCE, the oxidation peak current of RGO/GCE significantly increased due to the presence of the RGO film, which showed excellent electrical conductivity (curve c). When the AuNPs were deposited, the peak current was lower (curve d) than that of RGO/GCE. The lowest peak current and ΔE value were obtained. (curve e), which could be attributed to the Nafion membrane

acting as a blocking layer, impeding the diffusion of $[\text{Fe}(\text{CN})_6]^{3-/4-}$ towards the electrode surface[16]. The lower the ΔE value is, the better the reversibility of the redox reaction is.

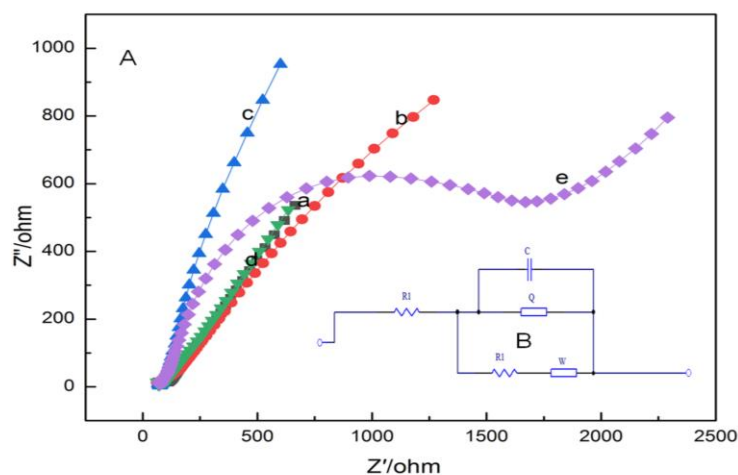


Figure 3. (A) EIS curves of (a) GCE, (b) GO/GCE, (c) RGO/GCE, (d) AuNPs/RGO/GCE, and (e) Nafion/AuNPs/RGO/GCE in 5.0 mM $[\text{Fe}(\text{CN})_6]^{3-/4-}$. (B) A Randle equivalent circuit.

Electrochemical impedance spectroscopy is an effective method for studying the interface properties of various electrodes and the electron-transfer resistance, as shown in Fig. 3. The results of cyclic voltammetry were consistent with those of AC impedance. These changes also showed that the Nafion/AuNPs/RGO/GCE membrane was successfully attached to the GCE surface.

On the basis of the Randles–Sevcik equation[17], $i_{pa} = 2.69 \times 10^5 n^{3/2} ACD^{1/2} v^{1/2}$, the electroactive surface area was estimated to be maximal on the RGO/GCE electrode. GO was electrochemically reduced to RGO by the current-time method (Fig. 4). The electrochemical reduction partially removed some of the oxygen-functional groups of GO and improved the electron conductivity of RGO. It can provide available active sites and expedite the penetration and diffusion of electrolyte ions [18-20].

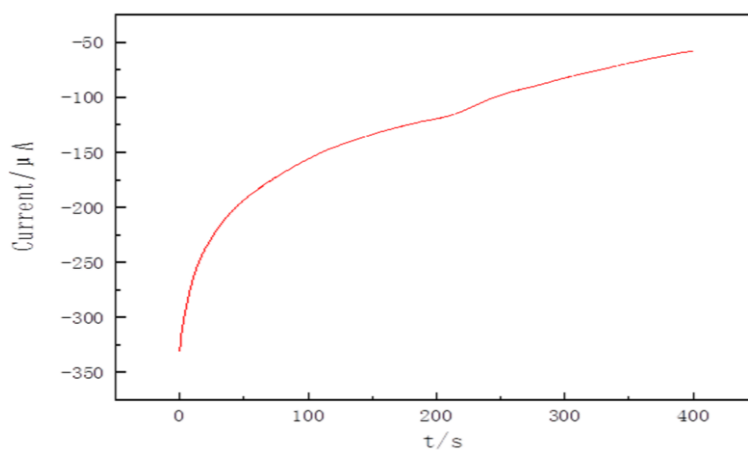


Figure 4. Current-time curve of electrochemical reduced graphene oxide (RGO) at pH=7.32 in a 0.1 M PBS solution at a potential of -0.9 V for 400 s

3.2. Characterization of AuNPs using SEM

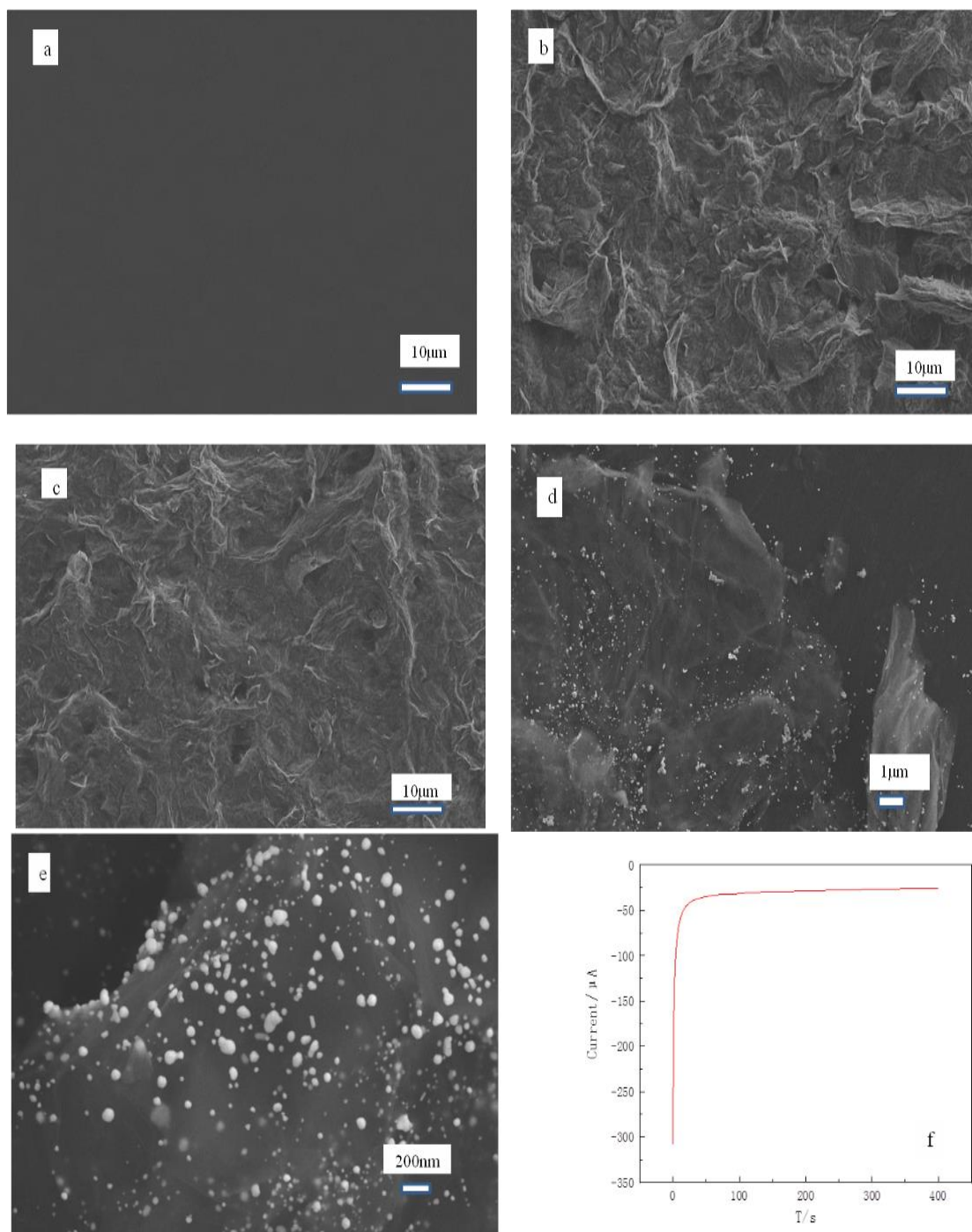


Figure 5. SEM of the different modified electrode surfaces. (a) GCE, (b) GO/GCE, (c) RGO/GCE, (d) AuNPs/RGO/GCE (1 μm), (e) Nafion/AuNPs/RGO/GCE (200 nm) (f) Current-time curve of electrodeposited gold nanoparticles

As shown in the SEM images in Fig. 5, the bare GCE had a smooth surface (a), whereas graphene oxide exhibited a typical wrinkled structure (b). Fig. 5 c shows the folded structure of the RGO sheets. A large number of AuNPs were homogeneously distributed on the RGO sheets (d). Immobilizing AuNPs on the surface of RGO prevented aggregation of RGO and effectively

increased the number of active sites [21,22]. At the same time, it enhanced the catalytic activity and the electron transport. The Nafion membrane was uniformly coated onto the surface of the electrode (e).

3.3 Electrochemical behaviour of diuron on Nafion/AuNPs/RGO/GCE

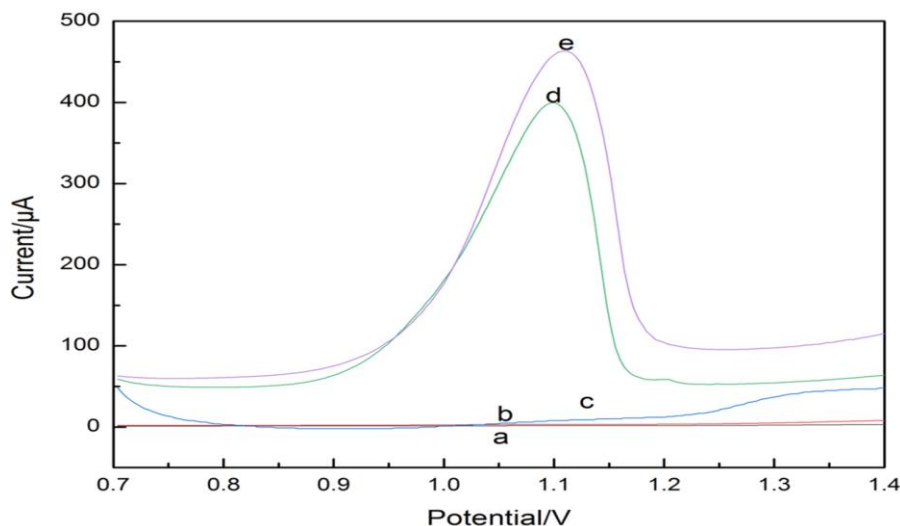


Figure 6. DPV of the electrochemical oxidation of 1.0×10^{-9} mol/L diuron at pH=4.50 in PBS solution on (a) GCE, (b) GO/GCE, (c) RGO/GCE, (d) AuNPs/RGO/GCE, (e) Nafion/AuNPs/RGO/GCE

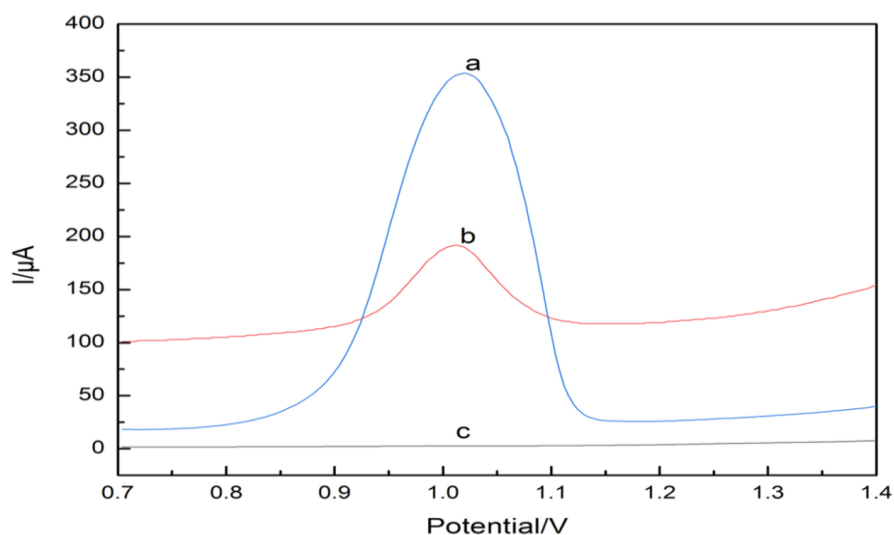


Figure 7. The differential pulse diagram on GCE (c) Nafion/AuNPs/RGO/GCE (a) with 1×10^{-9} mol/L and without diuron (b) at pH= 4.50 in PBS solution

As shown in Fig. 6, the oxidation peaks were almost nonrecognizable (curves a, b, c). Comparing the Nafion/AuNPs/RGO/GCE with the bare GCE, the current of the former was enhanced almost 4.5 times. Introducing AuNPs can separate graphene sheets and prevent them from

restacking. The synergistic effects of RGO and AuNPs improved the overall interfacial conductivity [21]. Diuron was assimilated from the solution onto the electrode surface by the high cation-exchange capacity of Nafion [16]. This incorporation resulted in the largest peak current of the modified electrode. So, a lower detection limit might be obtained.

In Fig. 7, Nafion/AuNPs/RGO/GCE resembled a very sensitive electrochemical sensor for the detection of diuron (curve a). Moreover, its peak current was approximately 300 times higher than that of the bare GCE. This result showed that the mixed membrane greatly expedited the electron transfer rate.

According to the Anson equation, the diffusion coefficient of diuron was estimated: $Q=2nFAD^{1/2}ct^{1/2}/\pi^{1/2}+Q_{dl}+Q_{ads}$, where A represents the electrode area, c denotes the concentration of diuron, n represents the number of moles ($n=2$), D denotes the diffusion coefficient, F is the Faraday constant, Q_{dl} and Q_{ads} represent the double layer charge and Faraday charge, respectively [23]. From the slopes of Q and $t^{1/2}$, the diffusion coefficient of diuron (D) was determined to be $2.498 \times 10^{-5} \text{ cm}^2/\text{s}$. This value was slightly larger than $6.43 \times 10^{-6} \text{ cm}^2/\text{s}$ on poly-Ni(OH)TAPc-GCE [24]. The results demonstrated that the electrode reaction of diuron was fast on Nafion/AuNPs/RGO/GCE.

3.4. Optimization of the detection conditions

To obtain the best performance of the Nafion/AuNPs/RGO/GCE electrode, we optimized the experimental parameters, including the solution pH, the AuNPs electrodeposition time and the resting time. The DPV curves in the 0.1 M PBS solution with $1 \times 10^{-9} \text{ M}$ diuron were recorded.

3.4.1 Effect of the solution pH

Because it has a very important effect on the sensitivity of the sensor, the solution pH (1.0-6.0) was varied (Fig. 8) and $\Delta I=I-I_0$ (I is the peak current in the mixed solution of PBS and diuron, and I_0 is the peak current in the blank solution) was measured as a function of pH. It could be seen that ΔI gradually increased with the increase in the pH value from 1.63 to 4.50. However, when the pH value was further increased, the peak current decreased. This phenomenon could be explained by the variation in electrostatic interactions. In more acidic solutions, positively charged diuron interacts with the anionic ionomer of Nafion on the electrode surface through ion-exchange and electrostatic attraction. Consequently, pH 4.50 was selected as a suitable pH in subsequent studies.

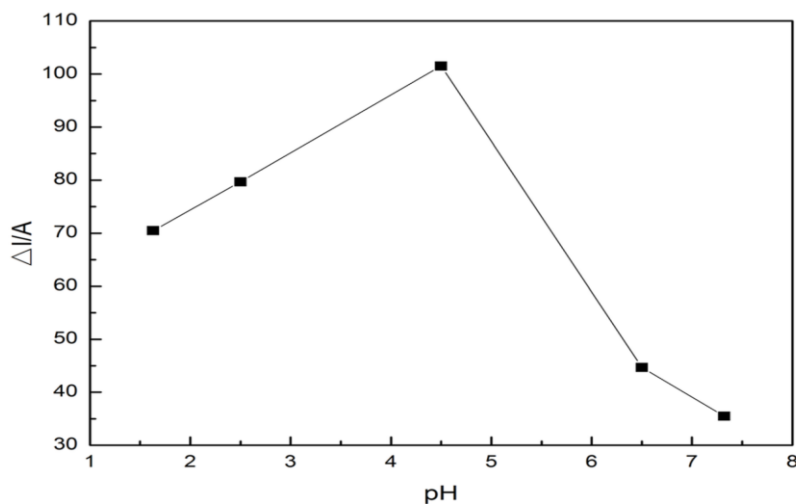


Figure 8. The polyline diagram of ΔI as a function of different pH values: (a) pH=1.63, (b) pH=2.50, (c) pH=4.50, (d) pH=6.50, (e) pH=7.32 in 0.1 M PBS with 1×10^{-9} mol/L diuron on Nafion/AuNPs/RGO/GCE.

3.4.2. Effect of gold nanoparticle electrodeposition time

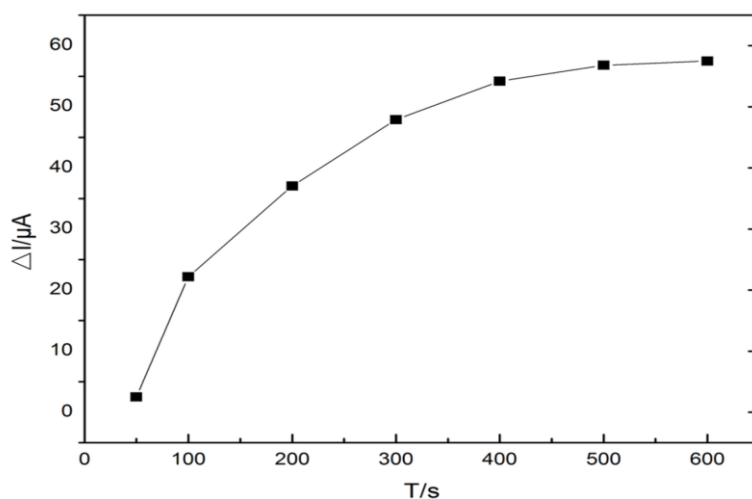


Figure 9. The polyline diagram of ΔI as a function of the deposition time of gold nanoparticles. (a) 50 s, (b) 100 s, (c) 200 s, (d) 300 s, (e) 400 s, (f) 500 s, (g) 600 s in 0.1 M pH=4.50 PBS with 1×10^{-9} M diuron on Nafion/AuNPs/RGO/GCE

Since the gold nanoparticle deposition time influences the analytical performance, varying deposition times were studied (Fig. 9). As the deposition time of gold nanoparticles increased, ΔI gradually increased. After 400 s, the peak current increased very slowly, mainly because most of the surface area of the modified electrode was covered at 400 s. Thus, 400 s of deposition time was chosen.

3.4.3. Effect of the resting time

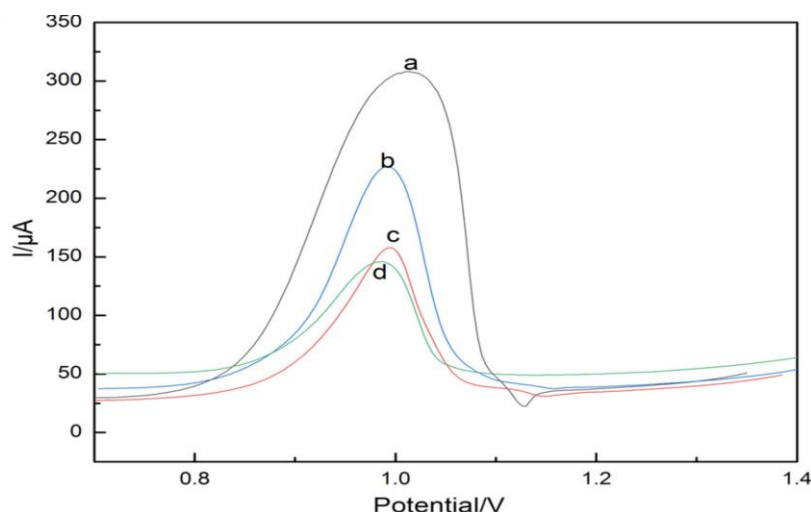


Figure 10. DPV graphs of different resting times. (a) 2 s, (b) 4 s, (c) 6 s, and (d) 8 s in 0.1 M pH=4.50 PBS with 1×10^{-9} M diuron on Nafion/AuNPs/RGO/GCE

The influence of resting time was surveyed. Fig. 10 shows that the peak current decreased with increasing resting time from 2 s to 8 s. When the resting time was 2 s, the peak current of the oxidation peak was the largest. Therefore, a resting time of 2 s was applied throughout the experiment.

3.5. Detection of diuron

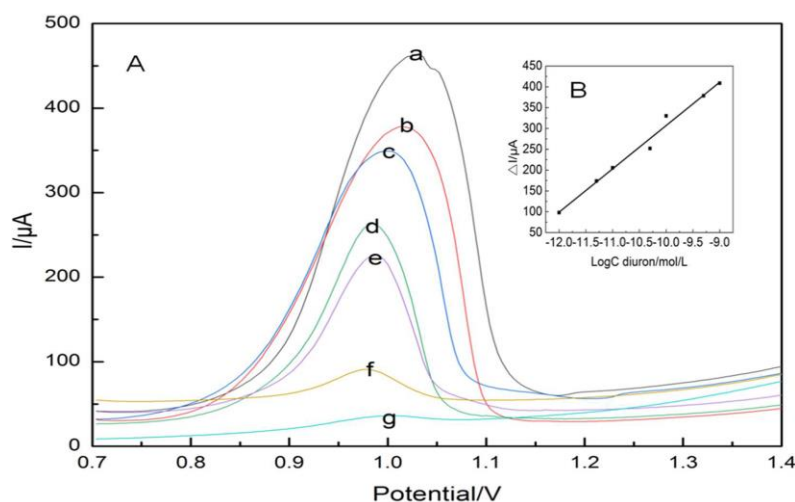


Figure 11. (A) DPV graphs of different concentrations of diuron: (a) 1.0×10^{-9} , (b) 5.0×10^{-10} , (c) 1.0×10^{-10} , (d) 5.0×10^{-11} , (e) 1.0×10^{-11} , (f) 5.0×10^{-12} , (g) 1.0×10^{-12} (B) The linear relationship between the logarithm of diuron concentration and ΔI .

Fig. 11A shows the DPV graphs of diuron at various concentrations on Nafion/AuNPs/RGO/GCE under the optimum conditions. A linear relationship of ΔI and the logarithm

of diuron concentration (lgc) was observed (Fig. 11B). ΔI was proportional to lgc from 1.0×10^{-12} M to 1.0×10^{-9} M. The linear equation was $\Delta I (\mu A) = 104.03 \text{ lgc (mol/L)} + 1347.3$. The detection limit (LOD) was 4×10^{-13} M. ($3\sigma/S$). Compared to the electrochemical analysis methods reported in the literature (Table 1), the present method had a lower detection limit.

Table 1. LOD of some works adopting different types of electrodes in the literature.

Voltammetric sensor	Analyte	LOD ($\mu\text{mol/L}$)	Reference
CPE modified by a complex to mimic the enzyme P450	diuron	36.14	25
GCE modified with polymerized nickelhydroxotetraamino-phthalocyaninein	diuron	0.33	24
Tetraamino-phthalocyanine iron (II)-single-walled carbon nanotubes	diuron	0.26	26
Molecularly imprinted polymer and carboxyl-functionalized multi-walled carbon nanotubes	diuron	9.0×10^{-3}	27
This method	diuron	4.0×10^{-7}	

3.6. Reproducibility, stability and selectivity

The reproducibility, stability and selectivity of Nafion/AuNPs/RGO/GCE were further evaluated. Five individual electrodes were used to evaluate the fabrication reproducibility. The relative standard deviation (RSD) for the detection of 1.0×10^{-9} M diuron was 3.69%, indicating that the method was highly reproducible due to the ease of preparation. Furthermore, after storing the presented sensor at 4°C , the current response retained 85% of its initial value after one week, indicating that the sensor had good storage stability. In addition, selectivity was carried out with 1.0×10^{-9} M diuron. Many coexisting substances, including Ca^{2+} , K^+ , Al^{3+} , Na^+ , Ba^{2+} , Ni^{2+} , Mn^{2+} , Cu^{2+} , Cl^- , NO_3^- , BrO_3^- , $\text{C}_2\text{O}_4^{2-}$, pyrocatechol and 1-nitroso-2-naphthol at 60 mg/L aminopyrene and nitropyrene at 50 mg/L (change rate of the peak current $<5\%$), did not affect the concentration of diuron even at 100 mg/L.

3.7. Real sample analysis

3.7.1. Sample treatment

A certain amount of dry tea was placed at 50°C in a ethyl alcohol/water mixture (15%) for 1 h and employed after filtration. Before use, a certain amount of pear juice was filtered to remove impurities. Mineral water was used directly.

3.7.2. Standard recovery experiment

To investigate the practical feasibility of the presented sensor, the applicability was surveyed in real samples of pear juice, tea water and mineral water by a standard addition method. The results are

shown in Table 2. The recoveries ranged from 91.2% to 108.2%, indicating that the method could be successfully applied for the determination of diuron in real samples.

Table 2. Recovery results of diuron by a standard addition method on Nafion/AuNPs/RGO/GCE

samples	Initial 10^{-10} mol/L	Added $\times 10^{-10}$ mol/L	Found $\times 10^{-10}$ mol/L	Recovery (%)
pear juice	ND	4.00	4.33 \pm 0.005	108.2
		4.50	4.77 \pm 0.007	105.9
		5.00	4.67 \pm 0.003	93.4
tea water	ND	4.00	3.69 \pm 0.006	92.3
		4.50	4.10 \pm 0.005	91.2
		5.00	5.13 \pm 0.006	102.5
mineral water	ND	4.00	3.90 \pm 0.005	97.6
		4.50	4.66 \pm 0.007	103.5
		5.00	5.27 \pm 0.004	105.3

ND: not detected

4. CONCLUSIONS

In summary, we constructed a very sensitive electrochemical sensor based on Nafion/AuNPs/RGO/GCE for the detection of diuron. The synergistic effects of the RGO and AuNPs composites as well as the effective absorption of diuron resulted in excellent interfacial conductivity. The combination led to a low detection limit. Under optimal conditions, the designed sensor showed high sensitivity, good selectivity and stable performance. Moreover, the method was successfully used in the quantitative determination of diuron in real samples. Therefore, it is expected to be applied to the detection of diuron in the environment in the future.

ACKNOWLEDGMENTS

Financial support from the National Natural Science Foundation of China (No. U1810110), the Applied Basic Research Programs of Science and Technology Department of Shanxi Province (No. 201901D211460), Shanxi Scholarship Council of China (No. 2020-140), The college students innovation and entrepreneurship project of Yuncheng University for featured agricultural products (No. XK-201957), Key Discipline Project of Applied Chemistry of Yuncheng University (No. XK-2019055, No. XK-201968, No. XK-201961) and Applied Research Project of Yuncheng College (No. XK-2019034) are gratefully acknowledged.

References

1. T. S. Anirudhan, F. Shainy and A. M. Mohan, *Sol. Energy*, 171 (2018) 534.
2. A. M. Polcaro, M. Mascia, S. Palmas and A. Vacca, *Electrochim. Acta*, 49 (2004) 649.
3. M. Pohanka, J. Fusek, V. Adam and R. Kizek, *Int. J. Electrochem. Sci.*, 8 (2013) 71
4. C. Lourencetti, M. R. R. Marchi, M. L. Ribeiro, *Talanta*, 77 (2008) 701.
5. L. E. V. Avila, B. P. M. Lira, M. Villanueva, R. Covarrubias, G. Zelada and V. Thibert, *Talanta*,

- 88 (2012) 553.
6. J. Liu, W. Cao, X. Yang and E. Wang, *Talanta*, 59 (2003) 453.
 7. H.Y. Xie, Y. Z. He, W. E. Gan, G. N. Fu, L. Li, F. Han and Y. Gao, *J. Chromatogr. A.*, 1216 (2009) 3353.
 8. P. Sharma, S. Gandhi, A. Chopra, N. Sekar and C. R. Suri, *Anal. Chim. Acta*, 676 (2010) 87.
 9. M. M. Galera, J. L. M. Vidal, A. G. Frenich and P. Parrilla, *Analyst*, 119 (1994) 1189.
 10. H. Wei, D.W. Pan, S. Ma, G. H. Gao and D. Z. Shen, *Analyst*, 144 (2019) 412.
 11. S. H. Li, Y. S. Ma, Y. K. Liu, G. Xin, M. H. Wang, Z. H. Zhang and Z. Y. Liu, *RSC Adv.*, 9 (2019) 2997.
 12. Y. Pang, *J. Electroanal. Chem.*, 769 (2016), 89.
 13. X. F. Niu, Y. B. Zhong, R. Chen, F. Wang, Y. J. Liu and D. Luo, *Sens. Actuators B*, 255 (2018) 1577.
 14. M. Govindhan and A. Chen, *J. Power Sources*, 274 (2015) 928.
 15. K. Zarei and H. Helli, *J. Electroanal. Chem.*, 749 (2015) 10.
 16. K. Zarei and A. Khodadadi, *Ecotoxicol. Environ. Saf.*, 144 (2017) 171.
 17. S. Rengaraj, Á. C. Izquierdo, L. Scott and M. D. Lorenzo, *Sens. Actuators B*, 265 (2018) 50.
 18. B. S. He and J. W. Li, *Anal. Methods*, 11(2019)1427.
 19. Z. Xiong, Z. D. Cheng, C. Yao, S. X. Zhong and M. A. Wei, *Chin. Sci. Bull.*, 57 (2012) 3045.
 20. Y. Shao, J. Wang, M. Engelhard, C. Wang and Y. Lin, *J. Mater. Chem.*, 20 (2010) 743.
 21. Z. Guo, Z. Y. Wang, H. H. Wang, G. Q. Huang and M. M. Li, *Mater. Sci. Eng.*, 57 (2015) 197.
 22. Y. Shao, H. Wang, J. Wu, I. Liu, A. Aksay and Y. Lin, *Electroanalysis*, 22 (2010) 1027.
 23. X. Xu, Q. Q. Zheng, G. M. Bai, L. S. Song, Y. W. Yao, X. D. Cao, S. Q. Liu and C. Yao, *Electrochim. Acta*, 242 (2017) 56.
 24. T. Mugadza and T. Nyokong, *Talanta*, 81 (2010) 1373.
 25. A. Wong, M. R. V. Lanza and M. P. T. Sotomayor, *J. Electroanal. Chem.*, 690 (2013) 83.
 26. T. Mugadza and T. Nyokong, *Electrochim. Acta*, 55 (2010) 2606.
 27. A. Wong, M. V. Foguel, S. Khan, F. M. Oliveira, C. R. T. Tarley and D. P. T. Maria, *Electrochim Acta*, 182 (2015) 122.